

Research Article

# Synthesis and Characterization of Cerium Metal Organic Frameworks (Ce-UiO-66) and Its Inorganic Hybrids

Dingetegna Godana Boynito<sup>1</sup>, Abi Tadesse Mengesha<sup>2,\*</sup> , Neelaiah Babu G.<sup>2</sup> 

<sup>1</sup>Department of Chemistry, College of Natural and Computational Sciences, Jinka University, Jinka, Ethiopia

<sup>2</sup>Department of Chemistry, College of Natural and Computational Sciences, Haramaya University, Haramaya, Ethiopia

## Abstract

Applications of metal-organic frameworks. Metal organic frameworks (MOFs) as exciting type of organic/inorganic hybrid materials have attracted great focus of scientists in the last two decades. The objective of this study was to synthesize Ce-UiO-66 and its inorganic hybrids (CdS/Ce-UiO-66/Ag<sub>3</sub>PO<sub>4</sub>) and characterize the synthesized cerium metal organic frameworks (Ce-UiO-66) and its inorganic hybrids. All the materials in this work were prepared via hydrothermal synthesis and characterized by X-ray powder diffraction (XRD) and scanning electron microscope (SEM) hyphenated with energy dispersive x-ray (EDX). From XRD data, peaks at 28.2, 29, 46.7 and 48.7 suggests the occurrence of CeO<sub>2</sub>. The three typical diffraction peaks observe at 2θ values of 26.67, 44.00 and 52.05 corresponding to miller indices of (100), (202) and (311) could be ascribed to the hawleyite structure of CdS. For the (1:1) ratio of CdS to Ce-Uio-66/Ag<sub>3</sub>PO<sub>4</sub> the XRD result reveal that the MOF structure disappeared making it more amorphous when compare to the other ratios. As the result, no diffraction peak attributable to Ag<sub>3</sub>PO<sub>4</sub> was observed. The scanning electron microscope (SEM) hyphenated with energy dispersive x-ray (EDX) analysis for all the inorganic hybrids reveal that all the distinct morphologies shown in their single phase vanished upon composite formation evidencing the well mix of each components. The EDX spectra in all cases show the presence of each component in the ternary system. Generally, in this research we focus on the synthesis of Ce-MOF and its inorganic hybrids and characterizations were studied. All the as-synthesized materials fall in the nanoscale.

## Keywords

Metal Organic Frameworks (MOFs), Inorganic Hybrids, Ce-UiO-66

## 1. Introduction

Metal organic frameworks (MOFs) represent a class of porous material which is formed by strong bonds between metal ions and organic linkers [1]. Metal-organic frameworks (MOFs) are highly versatile materials that find applications in several fields.

In recent decades, metal-organic frameworks (MOFs) have attracted widespread attention as an emerging class of porous

crystal materials, which are coordinated by metal ions/clusters and multifunctional organic ligands [2].

Nanoparticle/metal-organic frameworks (MOF) based composites have recently attracted significant attention as a new class of catalysts. Such composites possess the unique features of MOFs (including clearly defined crystal structure, high surface area, single site catalyst, special confined na-

\*Corresponding author: [abi92003@yahoo.com](mailto:abi92003@yahoo.com) (Abi Tadesse Mengesha)

**Received:** 10 October 2024; **Accepted:** 20 November 2024; **Published:** 17 January 2025



nopore, tunable, and uniform pore structure), but avoid some intrinsic weaknesses (like limited electrical conductivity and lack in the “conventional” catalytically active sites) [3]. To date many types of MOF composites have been developed to make use of the main aspects of MOF chemistry and to realize the full potential for their future utility. The increased number of materials that can be bound to each other (MOFs, hybrid materials, and nanocomposites) offers a chance to develop novel material properties [4-6].

Here we report on by synthesis of cerium metal-organic framework Ce-UiO-66 and its inorganic hybrids, CdS/Ce-UiO-66, Ce-UiO-66/Ag<sub>3</sub>PO<sub>4</sub>, and three different molar ratios of CdS to Ce-UiO-66/Ag<sub>3</sub>PO<sub>4</sub> of CdS/Ce-UiO-66/Ag<sub>3</sub>PO<sub>4</sub> (1:1, 0.75:1 and 0.5:1) MOF composites.

## 2. Materials and Methods

### 2.1. Experimental Work Site

All the synthesis and catalytic studies were conducted at the Chemistry Department Research Laboratory in Haramaya University. The characterizations, XRD and SEM-EDX were conducted in Madrid Spain.

### 2.2. Instruments and Apparatus

Different types of instruments and apparatus were used during the synthesis and characterizations of (Ce-MOF and its inorganic hybrids) Oven (Sanyo, OMT, U.K), centrifuge (HERMLE300, Germany), 1100 Hotplate and stirrer (Philip harris), magnetic stirrer, thermal balance, Furnace (Bibby Stuart, U.K), Sonicator (Kerry), X-ray diffractometer (XRD, Philips Analytical, PW-3040)), scanning electron microscopy (HITACHI Table top Microscope TM-1000), Kiesegel 60, 254, Merck, Germany), Petri dish, filter papers (Whatman No.1), sample holders, capillary tubes, melting point measuring instrument (Bibby Starling LTD, ST150SA model, U.K) analytical balance, pH-meter (MP220), mortar, crucible, test tubes, deionizer (HP143JH, U.K), distiller (Lasany, LPH-4, India), pipette, wash bottles, pyrex glass bottles and beakers.

### 2.3. Chemicals and Reagents

All chemicals and reagents were all of analytical grade. Cerium nitrate hexahydrate (Ce(NO<sub>3</sub>)<sub>3</sub>·6H<sub>2</sub>O, 99%), Terephthalic acid (H<sub>2</sub>BDC, 98%), concentrated HCl (BDH chemicals Ltd, England, 37%), Na<sub>2</sub>S·9H<sub>2</sub>O (Merck, Darmstadt, 99%), Cd(CH<sub>3</sub>COO)<sub>2</sub> (BDH, England, 99%), AgNO<sub>3</sub> (UNiChem, AR, 99.8%), Na<sub>2</sub>HPO<sub>4</sub> (BDH, England, 98%), Na<sub>2</sub>HPO<sub>4</sub>·12H<sub>2</sub>O (Guangdong, China, ≥ 99.0%), sodium hydroxide (NaOH), ethanol (Fine chemical, Ethiopia, 97%), and Ethyl acetate (99.9% CARLO EBRA, France).

## 2.4. Experimental Procedure

### 2.4.1. Synthesis of Ce-UiO-66

The synthesis of Ce-UiO-66 was carried out according to [7] with little modifications. Briefly, 4.3445 g (11.62 mmol) of Cerium nitrate hexahydrate salt (Ce(NO<sub>3</sub>)<sub>3</sub>·8H<sub>2</sub>O), 2.4803 g (14.92 mmol) of terephthalic acid (TPA) was dissolved separately in 50 mL of DIW. Then equimolar (1M) solution of ammonia with water was added into the linker solution drop by drop to deprotonate the organic acid completely though control of the pH. Next the metal salt solution was added to the linker solution with magnetic stirring for 1 h. The white precipitate formed was centrifuged at 2500 rpm for 20 min. The product was washed three times sequentially with DIW and ethanol then filtered. Finally the white colored solid was dried in an oven at 60 °C for 24 h and the material was designated as S1.

### 2.4.2. Synthesis of CdS /Ce-UiO-66

CdS/Ce-UiO-66 composites were prepared using the same method as used for the preparation of pure CdS with some modifications. 1.00 g each of UiO-66 and Cd(CH<sub>3</sub>COO)<sub>2</sub>·2H<sub>2</sub>O were dispersed in 50 mL of DIW. The suspension were transferred into an oven and heated at 100 °C for 12 h. After that, the products were cooled to room temperature, and the precipitates were collected by centrifugation and then purified with DIW and ethanol several times. The final products will be dried at 60 °C under vacuum. The obtained samples were labeled as CdS/UiO-66 [8, 9] and denoted as B1.

### 2.4.3. Synthesis of Ce-UiO-66/Ag<sub>3</sub>PO<sub>4</sub>

UiO-66 (Ce)/Ag<sub>3</sub>PO<sub>4</sub> composites were prepared via an in situ ion-exchange precipitation method with direct substitution of Cerium into Zr-MOF [10]. Firstly, 1.01 g as-prepared Ce-UiO-66 was dispersed in 100.0 mL of distilled water and sonicated for 30.0 min. Then, 1.0 g AgNO<sub>3</sub> was added and sonicated for another 30.0 min. After that, 0.7 g Na<sub>2</sub>HPO<sub>4</sub>·12H<sub>2</sub>O was dissolved in 10.0 mL of distilled water and added drop wise into the above solution under vigorous stirring. After stirring for 12 h, the final products were collected via filtration, washed with distilled water and ethanol three times and then dried under 60 °C in an oven for 2 h and denoted as B2.

### 2.4.4. Synthesis of Ternary CdS/UiO-66-Ce/Ag<sub>3</sub>PO<sub>4</sub>

The ternary nanocomposite CdS/UiO-66-Ce/Ag<sub>3</sub>PO<sub>4</sub> were prepared by taking 1.0 g of UiO-66-Ce/Ag<sub>3</sub>PO<sub>4</sub> nanocomposite with three different molar ratios of CdS versus UiO-66-Ce/Ag<sub>3</sub>PO<sub>4</sub>; i.e., 1:1, 0.75:1 and 0.5. Accordingly, the required amount of the binary composite was dissolved in 50 mL of deionized water and sonicate for 2 h. Next calculated amount of Cd(CH<sub>3</sub>COO)<sub>2</sub> was added and sonicated for additional 30 min. After this, stoichiometric amount of Na<sub>2</sub>S·9H<sub>2</sub>O

was dissolved in 50 mL deionized water and added to the above mixture then stirred vigorously for 12 h. Finally the blue black precipitate was collected and washed with deionized water and ethanol three times and lastly dried at 80 °C in oven for 6 h.

### 3. Results

#### 3.1. Synthesis of Nanomaterial's

In this work, CdS, Ag<sub>3</sub>PO<sub>4</sub>, Ce-MOF and its inorganic hybrids (CdS/UiO-66-Ce, UiO-66-Ce/Ag<sub>3</sub>PO<sub>4</sub> and CdS/UiO-66-Ce/Ag<sub>3</sub>PO<sub>4</sub>, with different molar ratio (1:1; 0.75:1 and 0.5:1) of CdS to UiO-66/Ag<sub>3</sub>PO<sub>4</sub>), were synthesized by precipitation and hydrothermal methods.

#### 3.2. Characterization Nanomaterial's CdS/UiO-66-Ce/Ag<sub>3</sub>PO<sub>4</sub>

The as-synthesized materials were then characterized by a variety of different techniques  
XRD Analysis

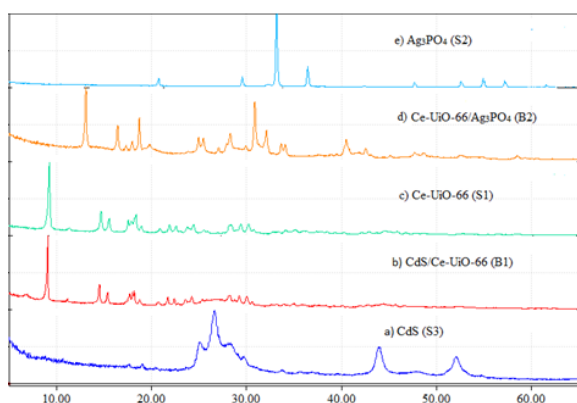


**Figure 1.** XRD Spectra of Ce-UiO-66, CdS, Ag<sub>3</sub>PO<sub>4</sub>, CdS/Ce-UiO-66 and Ce-UiO-66/Ag<sub>3</sub>PO<sub>4</sub>.

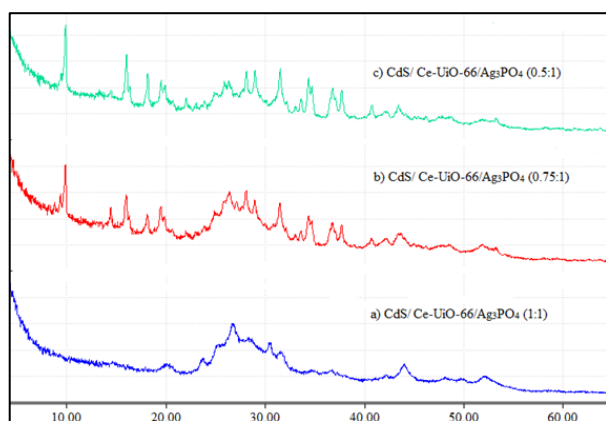


**Figure 2.** The XRD spectra of three different molar ratios of Cd:Ce in CdS/Ce-UiO-66/Ag<sub>3</sub>PO<sub>4</sub>(1:1(T1), 0.75:1(T2) and 0.5:1(T)).

The average crystallite size of the as-synthesized UiO-66(Ce-MOF) can be calculated using the Debye Scherrer formula;

$$D_s = 0.9\lambda / \beta \cos\theta \quad (1)$$

Where  $D_s$  = is the average crystallite size;  $\lambda$ = is the wavelength of the X-rays equals to 0.15406 nm corresponds to the Cu target  $K\alpha$  radiation;  $\beta$  = is the full width of half-maximum (FWHM) of an XRD, and  $\theta$  = is the Bragg diffraction angle in radians.

**Table 1.** Average crystallite sizes of the as-synthesized nanomaterials.

Sample	2 $\theta$ (degree)	$\beta$ (radians)	Ds (nm)
Ce-UiO-66	9.3	0.0035	39.6
CdS	26.48	0.0140	10.3
Ag <sub>3</sub> PO <sub>4</sub>	33.31	0.0035	40.8
CdS/Ce-UiO-66	9.03	0.0023	60.3
Ce-UiO-66/Ag <sub>3</sub> PO <sub>4</sub>	13.11	0.0035	39.6
CdS/Ce-UiO-66/Ag <sub>3</sub> PO <sub>4</sub> (1:1) (T1)	26.62	0.0257	5.5
CdS/Ce-UiO-66/Ag <sub>3</sub> PO <sub>4</sub> (0.75:1) (T2)	26.22	0.0245	5.8
CdS/Ce-UiO-66/Ag <sub>3</sub> PO <sub>4</sub> (0.5:1) (T3)	9.86	0.0023	60.3

All the as-synthesized materials fall in the nanoscale.

### 4. Discussions

The XRD pattern of CdS is shown in figure 1a. The three typical diffraction peaks observe at  $2\theta$  values of 26.67, 44.00 and 52.05 corresponding to miller indices of (100), (202) and (311) could be ascribed to the hawleyite structure of CdS [96-101-1261]. The result is in agreement to the literature reported [9]. The XRD pattern of Ag<sub>3</sub>PO<sub>4</sub> is shown in figure 1e. The apparent diffraction peak at around  $2\theta = 20.9^\circ, 29.7^\circ, 32.3^\circ, 33.3^\circ, 36.6^\circ, 38.1^\circ, 42.5^\circ$  are the confirmations for the existence of cubic structure of Ag<sub>3</sub>PO<sub>4</sub> [JCPD No.] impurity peaks were found indicating the formation of pure Ag<sub>3</sub>PO<sub>4</sub>. The sharp and narrow peaks indicate that Ag<sub>3</sub>PO<sub>4</sub> microcrystals are high purity and good crystallization [11-13].

As shown in Figure 1c, the most probable diffraction peaks for MOFs were found below scattering angle ( $2\theta$ ) of 10 and this is the characteristics of porous materials, which possess abundant pores or cavities. This means that; as the  $2\theta$  becomes less and less the material assumes a more porous

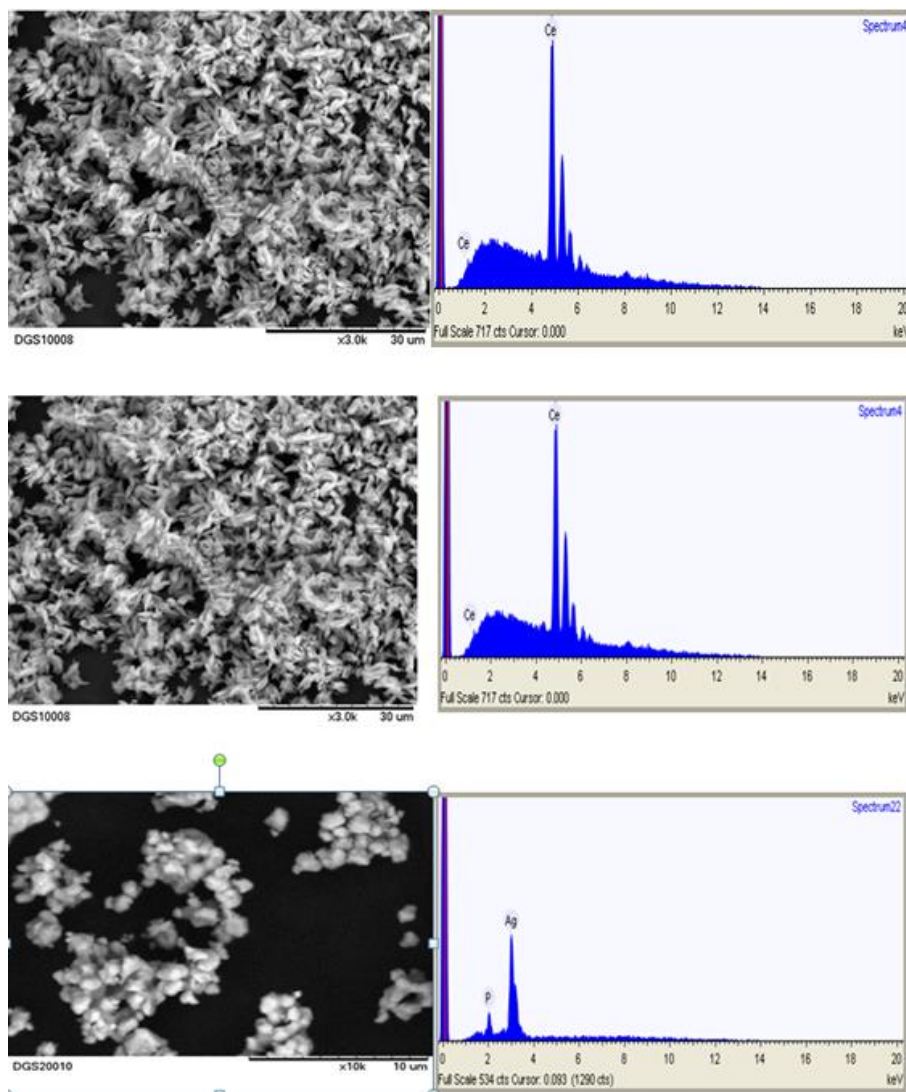
character and the more it has MOF's character. Thus, diffraction peaks, which are only found at  $2\theta$  closer to 10 and below were, selected [14]. The major peaks in the XRD patterns of UiO-66(Ce-MOF) is comparable with those reported on different literature [15, 16]. From XRD data, peaks at 28.2, 29, 46.7 and 48.7 suggests the occurrence of  $\text{CeO}_2$  [17, 18].

As presented in Figure 1b, the XRD patterns of the CdS/Ce-UiO-66 showed the peaks attributable to both. However, the major peak at  $2\theta$  value of 26.67 responsible for CdS appeared to be weak perhaps due to well dispersion of these crystals in the MOF pores. Otherwise all the major peaks are attributable to the Ce-MOF. In the case of Ce-UiO-66/ $\text{Ag}_3\text{PO}_4$  nanocomposite displayed in Figure 1d peaks attributable to both are also exhibited. In apparent contrast to the CdS/Ce-UiO-66 MOFs, major shift in peak position is noted in the case of Ce-UiO-66/ $\text{Ag}_3\text{PO}_4$ .

For the ternary systems, the general trend observed is the influence of CdS amount on the MOF structure. When the ratio of CdS to Ce-UiO-66/ $\text{Ag}_3\text{PO}_4$  reached 1:1, the MOF structure disappeared making it more amorphous and more like CdS than MOF composite. As the result, no diffraction peak attributable to  $\text{Ag}_3\text{PO}_4$  was observed. For the remaining compositions, the MOF structure is preserved. Besides, the peaks attributable to Ce-UiO-66,  $\text{Ag}_3\text{PO}_4$  and CdS are all observed.

#### SEM-EDX Analysis

The morphologies and elemental composition of as-prepared Ce-UiO-66 and its inorganic hybrids (CdS/ Ce-UiO-66, Ce-UiO-66/ $\text{Ag}_3\text{PO}_4$ , and CdS/Ce-UiO-66/ $\text{Ag}_3\text{PO}_4$  in various proportions were investigated by SEM-EDX (Figures 3a-h).



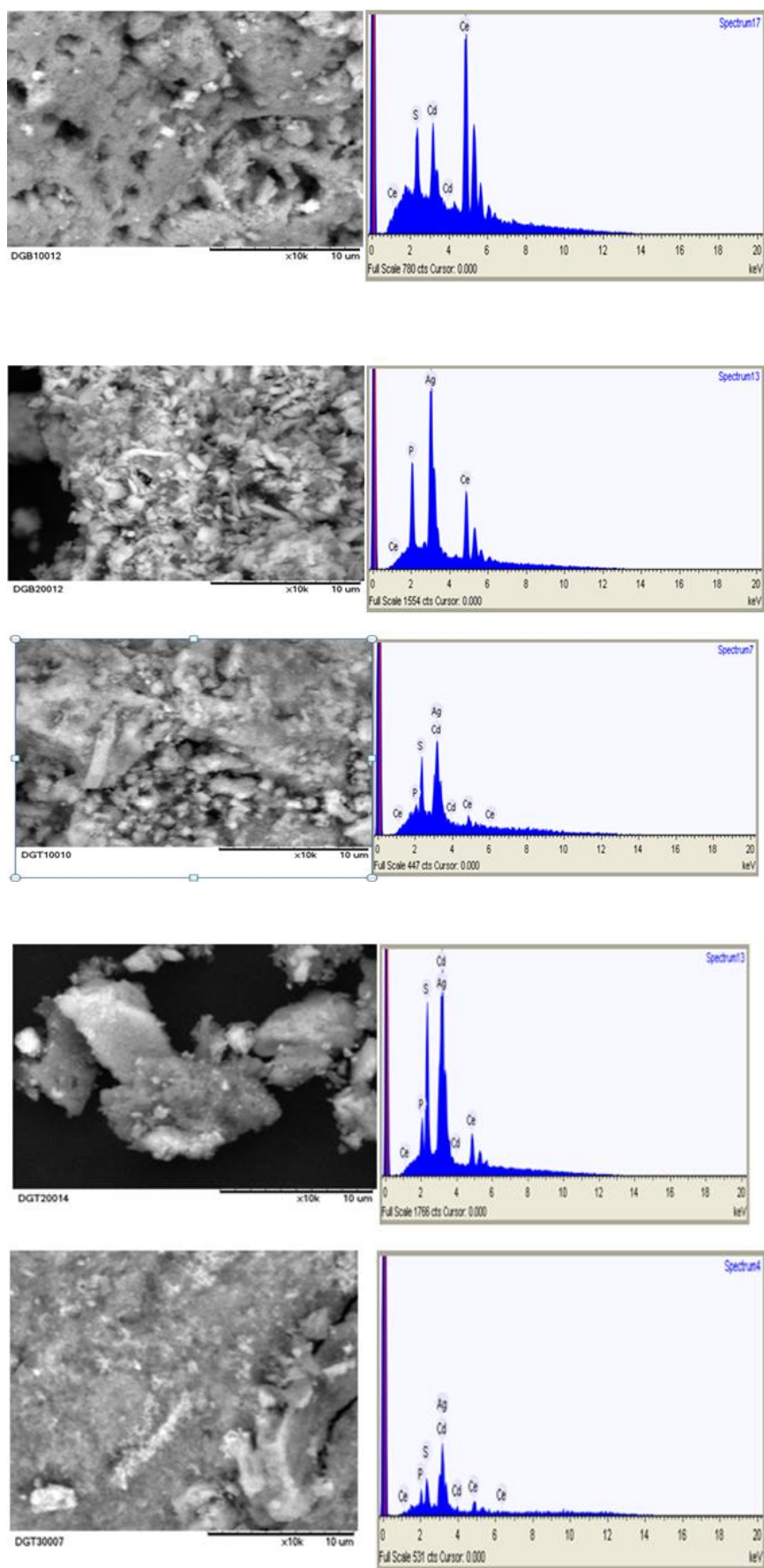


**Figure 3.** SEM micrograph of a) S1; b) S2 c) S3 d) B1 e) B2 f) T1 g) T2 h) T3 at high magnification and corresponding EDX spectra.

The SEM images Ce-UiO-66 products revealed rice like crystals with an average width  $\sim 100$  nm (Figure 3a). Moreover, a lot of small microcrystals with an average edge length of  $\sim 300$  nm were observed with uniform size distribution. It is clear from Figure 3b that the simple  $\text{Ag}_3\text{PO}_4$  are uniformly cubic-like in shape and uniformly distributed. The SEM micrograph of CdS revealed that there is the presence of well-structured and crystalline grains in the material (Figure 3c). When observed clearly at the micrograph obviously indicates the formation of hexagonal structure representing the greenockite like structure of the nanoparticles. The corresponding EDX spectrum for each single phase reveal the presence of only Ce for the Ce-UiO-66, Ag and P for  $\text{Ag}_3\text{PO}_4$  and Cd and S for CdS nanoparticles confirming the formation of pure phase with no impurity in all cases. For example, the average elemental percentage ratio of Cd:S was found to be 81.4% to 18.6% confirming almost a complete consumption of Cd precursor utilized and this is in good agreement with the result reported earlier [18].

For the binary system CdS/Ce-UiO-66, the SEM micrograph clearly exhibits the pore structure of the MOFs upon which crystals of CdS are deposited (Figure 3d). In contrast to this, the binary system comprising  $\text{Ag}_3\text{PO}_4$ /Ce-UiO-66 (Figure 3e) showed distinct rice like structure of the MOF intermingled with  $\text{Ag}_3\text{PO}_4$  crystals. The corresponding EDX spectra for both cases show the presence of all the components evidencing the purity of this phase although quite heterogeneous in the later case (Figure 3e).

For the ternary systems (Figure 3 f-h), all the distinct morphologies shown in their single phase vanished upon composite formation evidencing the well mix of each components. The EDX spectra in all cases show the presence of each component in the ternary system.

## 5. Conclusions

In this work, Ce-UiO-66, CdS,  $\text{Ag}_3\text{PO}_4$  and the inorganic hybrids of Ce-UiO-66; the binary and ternary systems were synthesized successfully by co-precipitation and a simple hydrothermal method at room temperature. The present method is advantageous as it does not involve any organic solvents and works at  $25^\circ\text{C}$  which complies with the Green Chemistry norms. Moreover, as-synthesized Ce-UiO-66, CdS,  $\text{Ag}_3\text{PO}_4$  and the inorganic hybrids of Ce-UiO-66 were characterized using PXRD and SEM-EDX. The XRD results revealed that as synthesized materials were Ce-UiO-66, CdS,  $\text{Ag}_3\text{PO}_4$  and the inorganic hybrids Ce-UiO-66 were all crystalline and the results matches with previously reported ones. The XRD result showed that CdS/Ce-UiO-66/  $\text{Ag}_3\text{PO}_4$  (1:1 and 0.75:1) and CdS have the smaller crystalline sizes compared to other as-synthesized material as shown in (Table 1). SEM micrograph showed cooked rice like particles for Ce-UiO-66 and cubic structures where observed for CdS.

## Abbreviations

XRD	X-ray Powder Diffraction
SEM	Scanning Electron Microscope
EDX	Hyphenated with Energy Dispersive X-ray

## Conflicts of Interest

The authors declare no conflicts of interest.

## References

- [1] Yap, M. H., Fow, K. L. and Chen, G. Z. 2017. Synthesis and applications of MOF-derived porous nanostructures. *Green Energy & Environment*, 2(3): 218-245.
- [2] Li, Y. Xia, T. Zhang, J. Cui, Y. Li, B. Yang, Y. Qian, G. (2019) A manganese-based metal-organic framework electrochemical sensor for highly sensitive cadmium ions detection, *Journal of Solid State Chemistry*. <https://doi.org/10.1016/j.jssc.2019.03.051>
- [3] Xiang, W., Zhang, Y., Lin, H. and Liu, C. J. 2017. Nanoparticle/metal-organic framework composites for catalytic applications: current status and perspective. *Molecules*, 22(12): 2103. <https://doi.org/10.3390/molecules22122103>
- [4] Kumar, P., Vellingiri, K., Kim, K. H., Brown, R. J. and Manos, M. J. 2017. Modern progress in metal-organic frameworks and their composites for diverse applications. *Microporous and Mesoporous Materials*, 253: 251-265. <https://doi.org/10.1016/j.micromeso.2017.07.003>
- [5] Jahan, M., Bao, Q., Yang, J. X. and Loh, K. P. 2010. Structure-directing role of graphene in the synthesis of metal-organic framework nanowire. *Journal of the American Chemical Society*, 132(41): 14487-14495.
- [6] Falcaro, P., Ricco, R., Yazdi, A., Imaz, I., Furukawa, S., Maspoeh, D., Ameloot, R., Evans, J. D. and Doonan, C. J. 2016. Application of metal and metal oxide nanoparticles@ MOFs. *Coordination chemistry reviews*, 307: 237-254. <https://doi.org/10.1016/j.ccr.2015.08.002>
- [7] Xiong, Y., Chen, S., Ye, F., Su, L., Zhang, C., Shen, S. and Zhao, S. 2015. Synthesis of a mixed valence state Ce-MOF as an oxidase mimetic for the colorimetric detection of biothiols. *Chemical Communications*, 51(22): 4635-4638. <https://doi.org/10.1039/C4CC10346G>
- [8] Shen, L., Luo, M., Liu, Y., Liang, R., Jing, F. and Wu, L. 2015. Noble-Metal-Free  $\text{MoS}_2$  CoCatalyst Decorated UiO-66/CdS Hybrids for Efficient Photocatalytic  $\text{H}_2$  Production. *Applied Catalysis B, Environmental*, 166-167: 445-53. <https://doi.org/10.1016/j.apcatb.2014.11.056>
- [9] Zhou, Y. 2015. Nanostructured cerium oxide based catalysts: synthesis, physical properties, and catalytic performance.

- [10] Xu, X. Y., Chu, C., Fu, H., Du, X. D., Wang, P., Zheng, W. and Wang, C. C. 2018. Light-responsive UiO-66-NH<sub>2</sub>/Ag<sub>3</sub>PO<sub>4</sub> MOF-nanoparticle composites for the capture and release of sulfamethoxazole. *Chemical Engineering Journal*, 350: 436–444. <https://doi.org/10.1016/j.cej.2018.06.005>
- [11] Guo, X., Chen, C., Yin, S., Huang, L. and Qin, W. 2015. Controlled synthesis and photocatalytic properties of Ag<sub>3</sub>PO<sub>4</sub> microcrystals. *Journal of Alloys and Compounds*, 619: 293–297. <https://doi.org/10.1016/j.jallcom.2014.09.065>
- [12] Wang, P. Q., Chen, T., Yu, B., Tao, P. and Bai, Y. 2016. Tollen's-assisted preparation of Ag<sub>3</sub>PO<sub>4</sub>/GO photo catalyst with enhanced photocatalytic activity and stability. *Journal of the Taiwan Institute of Chemical Engineers*, 62: 267–274. <https://doi.org/10.1016/j.jtice.2016.02.016>
- [13] Wang, P., Li, Y., Liu, Z., Chen, J., Wu, Y., Guo, M. and Na, P. 2017. In-situ deposition of Ag<sub>3</sub>PO<sub>4</sub> on TiO<sub>2</sub> nanosheets dominated by (001) facets for enhanced photocatalytic activities and recyclability. *Ceramics International*, 43: 11588–11595. <https://doi.org/10.1016/j.ceramint.2017.05.178>
- [14] Lin, A., Ibrahim, A. A., Arab, P., El-Kaderi, H. M. and El-Shall, M. S. 2017. Palladium Nanoparticles Supported on Ce-Metal-Organic Framework for Efficient CO Oxidation and Low-Temperature CO<sub>2</sub> Capture. *American Chemical Society: Applied Materials & Interfaces*, 9: 17961-17968. <https://doi.org/10.1021/acsami.7b03555>
- [15] Mosleha, S., Rahimia, M. R., Ghaedib, M., Dashtianb, K., Hajatic, S. and Wang, S. 2017. Ag<sub>3</sub>PO<sub>4</sub>/AgBr/Ag-HKUST-1-MOF composites as novel blue LED light active photocatalyst for enhanced degradation of ternary mixture of dyes in a rotating packed bed reactor. *Chemical Engineering and Processing*, 114: 24–38.
- [16] Tsegaye Girma. 2016. Synthesis and Characterization of UiO-66 Metal Organic Frameworks for Simultaneous Sorption of Methyl orange and Methylene blue from Aqueous Solution. MSc Thesis (*Unpublished*) Department of chemistry, Haramaya University, Ethiopia.
- [17] Haiyan, T., Yin, Z., Yunfan, Y., Weibing, H., Xinyu, S., Zhidou, T., Li, T. and Yin, Z. 2017. Preparation of Cerium Doped Cu/MIL-53(Al) Catalyst and Its Catalytic Activity in CO Oxidation Reaction. *Journal of Wuhan University of Technology-Material Science and Education*, 23: 1-6.
- [18] Mohammed Yimer. 2017. CdS-ZnS/ZTP Nanocomposite for Photocatalytic Degradation of Malachite Green Dye Under Ultraviolet and Visible Light Irradiations. MSc Thesis (*Unpublished*). Department of chemistry, Haramaya University, Ethiopia.